

Influence of polymer behaviour in organic solution on the production of polylactide nanoparticles by nanoprecipitation

Philippe Legrand^{a,b,1}, Sylviane Lesieur^{a,b,*}, Amélie Bochot^{a,b}, Ruxandra Gref^{a,b},
Wouter Raatjes^a, Gillian Barratt^{a,b}, Christine Vauthier^{a,b,**}

^a University Paris Sud, UMR CNRS 8612, IFR 141, Châtenay Malabry, F-92296, France

^b CNRS, UMR 8612, Châtenay-Malabry, F-92296, France

Received 5 March 2007; received in revised form 20 May 2007; accepted 23 May 2007

Available online 31 May 2007

Abstract

The aim of this study was to define the parameters determining an optimized yield of monodisperse, nanosized particles after nanoprecipitation of a biodegradable polymer, with a view to industrial scale-up the process. Poly(D,L)-lactides (PLAs) from a homologous series of different molar masses were nanoprecipitated at different initial polymer concentrations from two organic solvents, acetone and tetrahydrofuran (THF), into water without surfactant according to a standardized procedure. Quasi-elastic light scattering and gel permeation chromatography with universal detection were used respectively to size the particles and to determine the molar mass distribution of the polymeric chains forming both nanoparticles and bulk aggregates. The intrinsic viscosity of the polymers as a function of molar mass and solvent were determined by kinematic viscosity measurements in organic solutions. High yields of small nanoparticles were obtained with polymers of lower molar mass (22 600 and 32 100 g/mol). For a given polymer concentration in organic solution, the particle diameter was always lower from acetone than from THF. For initial molar masses higher than 32 100 g/mol, only dilute organic solutions gave significant yields of nanoparticles. Furthermore, polymer mass fractionation occurred with increasing initial molar mass and/or concentration: the nanoparticles were formed by polymeric chains of molar masses significantly lower than the average initial one. In general, nanoparticle production was satisfactory when the initial organic solution of polymer was in the dilute rather than the semi-dilute regime. Moreover, acetone, which acted as a theta solvent for PLA, always led to smaller particles and better yields than THF. © 2007 Elsevier B.V. All rights reserved.

Keywords: Nanoparticles; Sizing; Poly(D,L-lactic acid); Dilute solution regime; Production yield; Intrinsic viscosity

1. Introduction

The potential of polymer-based nanoparticles as drug delivery systems have been extensively investigated in recent years. They could provide a means of modifying the distribution of an

active substance in vivo and of increasing its concentration in the target tissue, thereby improving efficacy and reducing toxicity (Panyam and Labhasetwar, 2003; Moghimi et al., 2001; Brannon-Peppas and Blanchette, 2004). For these applications, the nanoparticles must not only be composed of a biodegradable and biocompatible polymer but also have a strictly controlled diameter and size distribution, particularly for intravenous administration (Jeon et al., 2000; Panyam and Labhasetwar, 2003). Indeed, the diameter of drug carriers is a crucial parameter determining the extent and rate at which they are removed from the circulation and their biodistribution (Juliano, 1976; Allen and Chonn, 1987). Particle size also affects drug loading and release.

Numerous methods for the manufacture of polymer nanoparticles have been described (De Jaeghere et al., 1999; Delair, 2004; Vauthier et al., 2004). In general, the process is critical in determining nanoparticle size (Lannibois et al., 1997; Jeon et al., 2000; Panyam and Labhasetwar, 2003). Among the

* Corresponding author at: Physico-chimie, Pharmacotechnie et Biopharmacie, UMR CNRS 8612, Université de Paris Sud, Faculté de Pharmacie, 92296 CHATENAY-MALABRY Cedex, France. Tel.: +33 1 46 83 53 49; fax: +33 1 46 83 53 12.

** Corresponding author at: Physico-chimie, Pharmacotechnie et Biopharmacie, UMR CNRS 8612, Université de Paris Sud, Faculté de Pharmacie, 92296 CHATENAY-MALABRY Cedex, France. Tel.: +33 1 46 83 56 03; fax: +33 1 46 83 53 12.

E-mail addresses: sylviane.lesieur@u-psud.fr (S. Lesieur), christine.vauthier@u-psud.fr (C. Vauthier).

¹ Present address: UMR CNRS 5618, Ecole Nationale Supérieure de Chimie de Montpellier, 104 rue de la Galera, 34097 Montpellier Cedex 5, France.

different methods, nanoprecipitation, which is simple, fast and economic, has the advantage of using preformed polymers as starting materials rather than monomers, as well as employing non toxic solvents (Fessi et al., 1989; Jain, 2000; Delair, 2004; Vauthier et al., 2004). It can also be applied to materials other than synthetic polymers, including amphiphilic cyclodextrins (Skiba et al., 1993; Lemos-Senna, 1998), proteins (Oppenheim, 1986; Duclairoir et al., 1998), lipids (Trotta et al., 2003) and drugs (Lannibois-Drean, 1995; Lannibois et al., 1997). For these reasons, this method is widely used to prepare nanoparticles for the delivery of active compounds.

To achieve nanoprecipitation, an organic solution of the polymer is simply added to a non-solvent of the polymer (generally water), with which the organic solvent is miscible. Nanoparticles form instantaneously by precipitation of the polymer in a narrow window of composition, after which the organic solvent can be removed by evaporation (Stainmesse et al., 1995). Under appropriate conditions, this technique leads to a dispersion of polymer particles that have a monomodal particle size distribution within the nanometer range, in a reproducible manner (Stainmesse et al., 1995; Molceperes et al., 1996; Govender et al., 1999; Lamprecht et al., 2001). Nanoprecipitation has been extended using quite complex systems containing the three basic ingredients (polymer, solvent, non-solvent) plus a surfactant and, sometimes, even a binary mixture of solvents of the polymer or a drug to be encapsulated (Niwa et al., 1993; Murakami et al., 2000; Chorny et al., 2002; Peltonen et al., 2003).

The choice of the ternary polymer/solvent/non-solvent system is critical for the success of the method. The nature of the polymer solvent interactions has been reported to affect the properties of the nanoparticle preparation (Thioune et al., 1997; Murakami et al., 2000; Galindo-Rodriguez et al., 2004). However, apart from the requirements that the polymer solvent should be miscible with the non-solvent of the polymer and that the polymer concentration should be low (<2%), no clear guidelines about the influence of each of the three components of the system have yet emerged. Some experimental work has attempted to investigate the effect of several parameters on the size of nanoparticles prepared with different polymers and solvents and on the yield of nanoparticle production (Stainmesse et al., 1995; Thioune et al., 1997; Murakami et al., 2000; Galindo-Rodriguez et al., 2004). In general, by increasing the polarity of the polymer solvents and by decreasing concentration of the polymer in the solvent the yield of nanoparticle production can be increased and the size of the nanoparticles reduced. These studies have also pointed out the importance of the solvency properties of the solvent of the polymer in the control of nanoprecipitation process. In this respect, Thioune et al., 1997 suggested investigating the intrinsic viscosity of the polymer dissolved in the chosen solvent and determining the Huggin's interaction constant, but otherwise stated, no such study has been yet performed.

The purpose of our work was to study the relationship between polymer-solvent interactions and the size of the nanoparticles obtained by nanoprecipitation and on the yield of nanoparticle production. A standardized process using defined and controlled operating conditions was developed so that

the characteristics of the polymer and of the polymer solution remained the main parameters influencing nanoprecipitation. In order to further simplify the system, no stabilizing agent was used.

The polymer selected was a polyester, poly(lactic acid), available in different molar masses. This polymer is widely used in the form of bioresorbable drug delivery systems or devices in surgery and pharmacology due to its excellent biocompatibility and biodegradability and because it is approved by the United States Food and Drug Administration for drug delivery (Jain et al., 1998; Södergård and Stolt, 2002; Panyam and Labhasetwar, 2003). It is also the polymer most commonly chosen to produce nanoparticles by nanoprecipitation (Jain, 2000; Lu and Chen, 2004). The choice of two appropriate solvents was made on the basis of their physico-chemical properties, as explained below.

2. Theoretical considerations for the choice of the solvents for the polymer

The choice of two solvents suitable for the nanoprecipitation of PLA was based on the requirements of the method and on the physico-chemical characteristics of this polymer. The method dictates that the organic solvents must be able to dissolve PLA. They must also be miscible with water and have a low boiling point to facilitate their elimination by evaporation. Taking into account these criteria, solvents were selected to allow the effects of polymer-solvent interactions to be investigated. The main physico-chemical parameters which may influence such interactions are those defining the polarity of the solvent. In our study, two solvents were chosen which only differed by their polarity. These were acetone, which is widely used in nanoprecipitation of polyesters including PLA, and THF (Fessi et al., 1989; Belbella et al., 1996; Govender et al., 1999; Gref et al., 2000, 2003; Le Roy Boehm et al., 2000; Leo et al., 2004). Table 1 gives their main physico-chemical properties and shows that the main differences between the two solvents are to be found in their dielectric constant and dipole moment. The solubility parameters of acetone and THF are quite similar except for the partial solubility parameter attributed to the polar forces (δ_p) which is twice as high for acetone as for THF. Therefore, acetone is more polar than THF. The partial solubility parameters of PLA were calculated according to the Van Krevelen group contribution method based on the classical Hansen solubility parameter method (Van Krevelen and Hoftyzer, 1976). The values reported in Table 1 are in good agreement with those recently calculated by Agrawal et al., 2004. The partial solubility parameters of PLA were compared with those of water, acetone and THF on a Bagley's two-dimensional graph (Bagley et al., 1971) (Fig. 1). This graph is useful for predicting whether a given solvent will be a solvent or a non-solvent of a polymer because solvents of a polymer are generally included in a circle of a radius of five δ -units around the polymer (Bagley et al., 1971; Sung and Lee, 2001). As expected, water appeared far outside the solubility circle of PLA, in agreement with the fact that it is a non-solvent of this polymer. THF and acetone were located near each other on the edge of the solubility circle (Fig. 1). This indicates that they should both be good solvents

Table 1
Physico-chemical characteristics of the solvents and of the polymer used in the preparation of nanoparticles

Parameter	Water	Acetone	THF	PLA ^a	PLA ^b
Dielectric constant	80.37	21.0	7.5		
Dipole moment (debye)	1.84	2.7	1.6		
Solubility parameters (J/cm ³) ^{1/2}					
$\delta_t = (\delta_d^2 + \delta_p^2 + \delta_h^2)^{1/2}$	48.08	19.99	19.48	23.31	21.73
$\delta_d = \sum F_{di}/V$	12.28	15.51	16.82	17.62	18.50
$\delta_p = (\sum F_{pi}^2)^{1/2}/V$	31.30	10.43	5.73	9.70	9.70
$\delta_h = (-\sum U_{hi}/V)^{1/2}$	34.17	6.96	7.98	11.77	6.00
$\delta_v = (\delta_p^2 + \delta_d^2)^{1/2}$	33.62	18.69	17.77	20.12	20.89
Boiling point (°C)	100	56.3	81.6		
Density 20 °C	1.000	0.791	0.8892		
Viscosity 20 °C (Cp)	1.002	0.324	0.486		
Surface tension γ 10 ⁻³ (J/m ²)	71.98	22.68	26.4		

The partial solubility parameters of the solvents were taken from tables (Burrell, 1975). δ solubility parameter, subscripts t, total; d, contribution of the dispersion forces; p, polar contribution; h, hydrogen bonding contribution; v, dispersion and polar contribution. V , molar volume of the compound; F_{di} , molar attraction constant due to dispersion interactions; F_{pi} , molar attraction constant due to polar interactions; U_{hi} , hydrogen bond energy.

^a Calculation of the partial solubility parameters of PLA by the Van Krevelen group contribution method based on the classical method for Hansen solubility parameters (Van Krevelen and Hoftyzer, 1976).

^b Taken from Agrawal et al., 2004, calculated by the Van Krevelen group contribution optimization method.

for PLA. It can also be expected that the interactions of these solvents with water will be very similar because they are clustered in a small area of the graph. Thus, in ternary systems consisting of either PLA/acetone/water or PLA/THF/water the difference

in the interactions between the organic solvent and water might be negligible. This would allow to study in more details the influences of parameters related only to the polymer and to the polymer–solvent interactions on nanoprecipitation.

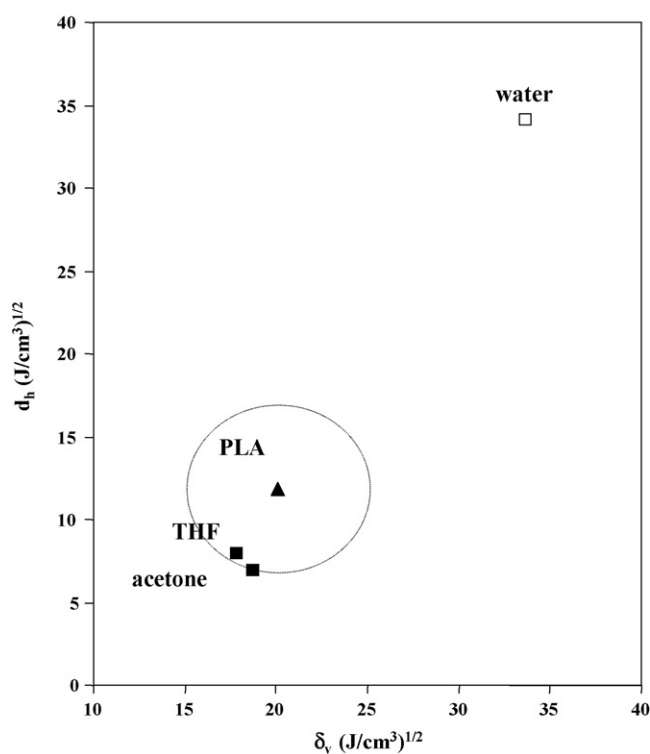


Fig. 1. Bagley's two-dimensional graph of the partial solubility parameters of the solvents with respect to the partial solubility parameters determined for PLA. (▲), PLA; line (· · ·), limit of the solubility circle of PLA; (■), solvents of PLA; (□), non-solvent of PLA.

3. Materials and methods

3.1. Chemicals

Acetone (for ACS-ISO-for analysis, purity >99.8%) and tetrahydrofuran (THF) (for HPLC, purity >99.8%) were supplied by Carlo Erba. For the aqueous phase, distilled water produced by reverse osmosis (MilliQ[®], Millipore) was used.

Poly-DL-lactic acid (hereafter referred to as PLA) species with $M_w = 22600$ g/mol, IP 3.5 (PLA₂₂₆₀₀), $M_w = 32100$ g/mol, IP 3.4 (PLA₃₂₁₀₀), $M_w = 52300$ g/mol, IP 3.9 (PLA₅₂₃₀₀), $M_w = 54400$ g/mol, IP 4.5 (PLA₅₄₄₀₀), $M_w = 93700$ g/mol, IP 4.0 (PLA₉₃₇₀₀), $M_w = 106300$ g/mol, 4.2 (PLA₁₀₆₃₀₀), $M_w = 124800$ g/mol, IP 4.3 (PLA₁₂₄₈₀₀) were supplied by Phusis (France). The molar masses are weight average molar mass as checked by gel permeation chromatography (GPC) as described below.

4. Determination of the molar mass of the polymers by high-performance gel permeation chromatography (GPC)

The molar masses of the polymers were determined by GPC with a ViscoGEL column, type GMHHR-M mixed bed, 7.8 mm × 300 mm (Viscotek, Houston, Texas, US) preceded by a ViscoGEL type HHR-H guard column, 6 mm × 40 mm (Viscotek, Houston, Texas, US). The apparatus included a VE 7510 degasser (Viscotek, Houston, Texas, US), a VE 1121 pump (Vis-

cotek, Houston, Texas, US), an automatic 712 WISP injector (Waters, Saint-Quentin en Yvelines, France), and was equipped with triple detection including a Waters 410 differential refractometer and a viscosimeter coupled with the measurement of the light scattered at 90° (T60A, Viscotek, Houston, Texas, USA). The column was maintained at a temperature of 40 °C using a Waters TCM heating column system. THF was used as the eluant at a flow rate of 1 ml/min. Toluene solution in THF (5:100, v/v) was used as an internal standard (retention time = 12.5 ± 0.1 min). Before injection all samples were filtered using a PTFE membrane (Millex-FG, 0.2 mm × 4 mm, Millipore, St. Quentin France). The injection volume was 100 µl.

The column was calibrated using polystyrene standards of different molar masses: 580, 925, 1270, 1940, 2960, 5000, 7200, 13100, 21000, 37900 g/mol, purchased from Polymer Laboratories (Shropshire, UK), 9100, 18100, 117000, 355000 g/mol, supplied by TSK standard Tosoh (Tokyo, Japan) and 90000 obtained from Viscotek (Houston, Texas, US). Solutions of standard polystyrene were prepared by the dissolution of the polymers in THF at a concentration ranging from 1 to 7 mg/ml depending on the molar mass. A universal calibration curve was drawn with the help of the TriSEC 3.0 GPC software from Viscotek (Houston, Texas, US).

PLA was dissolved in THF at a concentration of 5 mg/ml. For the determination of the molar mass of the PLA recovered in the different fractions isolated from the nanoprecipitation experiments, the polymers were dissolved in THF at concentrations ranging from 1 to 5 mg/ml depending on the amount of polymer available.

4.1. Viscosity measurements

All PLA solutions studied were prepared in class A volumetric flasks and allowed to reach equilibrium for 18 h at 20 °C before measurement. Polymer contents were determined by weight ($\pm 2 \times 10^{-5}$ g).

Prior to kinematic viscosity investigations, the rheological behaviour of PLA solutions in acetone or THF was characterized with a Rheostress RS100 5 Ncm apparatus (Haake Fisons, Karlsruhe, Germany) using a DG41 R&S cylindrical coaxial geometry. Experiments were performed at 22 °C by raising the shear stress from 0 to 2 Pa before reducing it to 0 Pa over a fixed period of 600 s. This corresponded to shear rates varying from 0 up to 3000 s⁻¹ depending on both PLA molar mass and concentration. Curves of shear stress versus shear rate were computed using the Rheowin Job Pro & Data software. Organic solutions of 1–50 mg/ml PLA with M_w between 22600 and 124800 g/mol showed linear behaviour (data not shown). In these molecular mass and concentration ranges, PLA solutions thus exhibited constant dynamic viscosities and behaved as Newtonian liquids that allowed capillary viscosity measurements.

The kinematic viscosities of the solvents (ν_0) and polymer solutions (ν) were determined at 22 °C, using a temperature-controlled capillary viscosimeter CK 100 (Schott-Geräte, Mainz, Germany) equipped with a microcapillary Ubbelohde tube (9.969×10^{-3} mm² s⁻² flow-time constant; Schott-Geräte,

Mainz, Germany). The viscosity of each solution was calculated from the average of five repeated measurements. The precision of separate mean values was estimated as 10% from duplicate determinations performed on independent solutions of the same concentration. The viscosities of the PLA solutions were measured in 1–20 mg/ml concentration range to ensure both Newtonian flow conditions and only a small difference in density from the solvent, so that specific viscosity η_{sp} could be calculated according to equation:

$$\eta_{sp} = \frac{(\nu - \nu_0)}{\nu_0} \quad (1)$$

Although some of the viscosity parameters can be deduced from GPC by the use of the triple detection method, for consistency within the work, all viscosity parameters were deduced from measurements performed using the capillary viscosimeter on PLA solutions in THF and in acetone.

4.2. Nanoprecipitation setup

The experimental protocol was designed to ensure reproducible conditions by fixing the stirring speed, the mode of solvent addition, the temperature and the aqueous to organic volume ratio and using the same glassware and stirring bar. All equipment was pre-weighed before use in order to determine the masses of polymer lost at each stage of the process.

The initial concentrations of PLA in the organic solution (THF or acetone) were: 5, 10, 15, 20 mg/ml. The organic phase to aqueous phase ratio was 1:2 (4.5 ml/9 ml). The volumes of THF or acetone were determined by weight on the basis of their densities. Organic solutions of PLA were equilibrated for 18 h at room temperature and maintained for 1 h at 22 °C before nanoprecipitation.

Nanoprecipitation was performed at 22 °C by continuously pouring 4.5 ml PLA organic solution through a needle (0.9 mm internal diameter) connected to a glass reservoir of 5 ml into 9 ml of aqueous phase placed in the pre-weighed 50 ml round bottom flask. Complete addition was achieved within 1 min. The mixture was maintained under magnetic stirring at 300 rotations per minute during the addition of the organic phase and for a further 10 min, using an identical stirring bar for every preparation. Organic solvent was then completely removed by evaporation under reduced pressure (Rotavapor) at a constant temperature of 22 °C (acetone) or 28 °C (THF).

The crude nanoparticle suspensions were centrifuged at $1500 \times g$ for 15 min at 20 °C to separate nanoparticles, which remained in the supernatant, from larger polymer aggregates (Centrifuge Jouan CR412). The PLA fractions (nanoparticles, polymer aggregates) were freeze-dried separately (freeze dryer Christ loc-1 Alpha1-4, Bioblock Scientific) and analysed by GPC as described above to determine the molar mass of the polymer present.

The yields of nanoparticles (NP) and aggregates (Agg) from three independent experiments for each preparation were determined by weighing the dry different fractions (balance precision 10^{-4} g) and calculated as follows as weight percent with respect

to the total recovered polymer (M_{total}).

$$\text{NP}(\%) = \frac{M_{\text{NP}}}{M_{\text{total}}} \times 100 \quad \text{with } M_{\text{total}} = M_{\text{NP}} + M_{\text{Agg}} \quad (2)$$

$$\text{Agg}(\%) = \frac{M_{\text{Agg}}}{M_{\text{total}}} \times 100 \quad (3)$$

The mass of nanoparticles (M_{NP}) was determined by weighing the material recovered from the supernatant after freeze-drying. The mass of the aggregates (M_{Agg}) formed during the nanoprecipitation process was deduced from all polymeric fractions which were not nanoparticles (pellet recovered after centrifugation, polymer stuck to the magnetic stirrer and flask bottom: measured by weighing after use).

4.3. Quasi-elastic light scattering

Mean hydrodynamic diameters (d_{H}) and polydispersity of the nanoparticles recovered in the supernatant after centrifugation were evaluated by quasi-elastic light scattering (QELS) with a Coulter Nanosizer NS (Beckman-Coulter, Margency, France) after adequate dilution with MilliQ[®] water. The hydrodynamic diameter of the particles was calculated according to the Stokes–Einstein law.

For each sample, the measurement was made three times with data acquisition for 120 s, at a temperature of 20 °C and with a detection angle of 90°. The polydispersity index I_{p} of the nanoparticles was always between 0 and 0.3; therefore, these preparations could be assumed to be monodisperse and the d_{H} value was calculated using the “Unimodal” method.

5. Results

5.1. Intrinsic viscosity

Before comparing the efficiency of PLA at forming nanoparticles as a function of the nature of the organic solvent and chain length, it was necessary to ensure that the different PLA species studied were homologous in chemical structure, independently of their molar mass. This was verified by performing kinematic viscosity measurements in the two organic solvents chosen for the study. A second purpose of these measurements was to evaluate the polymer–solvent interactions to verify that acetone and THF were “good” solvents for PLA as suggested by their solubility parameters (Fig. 1, Table 1). Plots of reduced viscosity η_{sp}/C versus polymer concentration C are shown in Fig. 2a and b as a function of PLA molar mass for each solvent. The linear relationships observed are in agreement with Huggin’s equation characterizing dilute solutions of macromolecules (Huggins, 1942):

$$\frac{\eta_{\text{sp}}}{C} = [\eta] + k'[\eta]^2 C \quad (4)$$

where $[\eta]$ and k' are the intrinsic viscosity and the interaction constant, respectively. Linear regression analyses of the curves gave $[\eta]$ by extrapolating the η_{sp}/C value to zero concentration while k' values were calculated from the slopes of the lines (Table 2). It is worth noting that each series of PLA solutions led to an almost constant Huggin’s coefficient k' . This result confirmed that the polymers used in this study possessed a similar chemical structure and their interactions with acetone or THF were independent of their chain length. Moreover, the values of

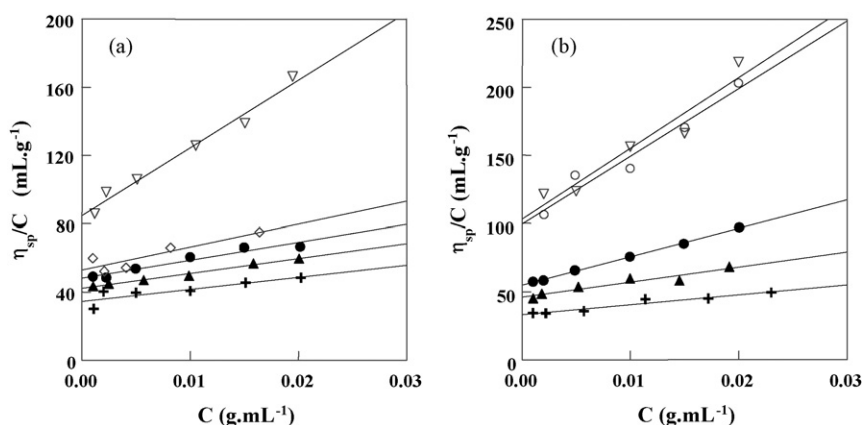


Fig. 2. Variation of reduced viscosity as a function of PLA concentration in acetone (a) and THF (b) at 22 °C and polymer molar mass (g/mol): 22600 (+), 32100 (▲), 54400 in acetone and 52300 in THF (●), 93700 (◇), 106300 (○), 124800 (▽).

Table 2

PLA intrinsic viscosities $[\eta]$ (mL g^{-1}) as a function of solvent and molar mass at 22 °C

	PLA ₂₂₆₀₀	PLA ₃₂₁₀₀	PLA ₅₂₃₀₀	PLA ₅₄₄₀₀	PLA ₉₃₇₀₀	PLA ₁₀₆₃₀₀	PLA ₁₂₄₈₀₀	k'^a
Acetone	32.4	42.2	–	48.1	52.9	–	84.7	0.5 ± 0.1
THF	33.1	46.1	54.9	–	–	99.4	103.1	0.6 ± 0.1

(–), Not determined.

^a Mean Huggin’s interaction constant calculated from linear regression analyses of η_{sp}/C vs. C plots (Fig. 2) and Eq. (4).

0.5 and 0.6 found for k' were characteristic of flexible polymers in fairly good solvents (Riesemann and Ullman, 1951). THF appeared to be slightly less efficient at solubilizing PLA than acetone.

The variations of the intrinsic viscosities versus polymer molar masses followed power-law relationships in agreement with Mark–Houwink's equation (Flory, 1953):

$$[\eta] = KM^\alpha \quad (5)$$

where the parameters K and α are characteristic of the polymer–solvent system. Interestingly, log–log plots of $[\eta]$ versus M_w led to α values close to 0.5 and 0.7 for the PLA–acetone and PLA–THF systems, respectively. This confirmed that both are good solvents for PLA. Nevertheless the Mark–Houwink's exponent of 0.5 in acetone indicated Flory theta solvent conditions so that PLA chains can be expected to behave as “ideal coils” (Flory, 1969) in the solvent.

5.2. Yield of fabrication and size of nanoparticles

When the organic solution of PLA was added to water, the mixture immediately became turbid, indicating the formation of nanoparticles. However, depending on the conditions, the final suspension also contained a larger or smaller amount of larger polymeric aggregates either dispersed in the aqueous phase or adhering to the flask wall or to the magnetic stirring bar. The effective yield of nanoparticles was then more or less affected by this bulk precipitation phenomenon.

First of all, it is worth noting that measurements of nanoparticle yield and size made on three different batches produced under identical conditions fell within a range of 10%, indicating the good reproducibility of the standardized nanoprecipitation process. The yield of nanoparticles depended on the nature of the organic solvent, the molar mass and concentration of the polymer. Higher nanoparticle yields were always obtained from acetone solution than from THF solution at equivalent polymer molar mass and concentration (compare Fig. 3a and b).

With PLA₂₂₆₀₀ and PLA₃₂₁₀₀ in acetone solution, the concentration of polymer did not influence the yield of nanoparticles formed that was always more than 70% (Fig. 3a). Maximum production was reached at 20 mg/ml initial PLA and corresponded to a production of 63 mg PLA as nanoparticles (Fig. 4a). However, at higher molar mass the yield decreased with increasing polymer concentration. This effect was extremely marked with PLA₁₂₄₈₀₀. In contrast, in THF solution, the influence of polymer concentration on nanoparticle yield was observed even at low molar mass (Fig. 3b). It was even more pronounced at high molar mass. The fabrication yield fell below 50% at polymer concentrations above 10 mg/ml especially with polymers of molar masses higher than 32100 g/mol. No more than 40 mg of PLA nanoparticles were recovered from 90 mg of PLA when THF was the solvent (Fig. 4b) in contrast to 63 mg of nanoparticles produced from 90 mg of PLA dissolved in acetone (Fig. 4a).

In general, the mean hydrodynamic diameter of nanoparticles increased with increasing molar mass and polymer concentration (Fig. 5a and b). This relationship was more pronounced with

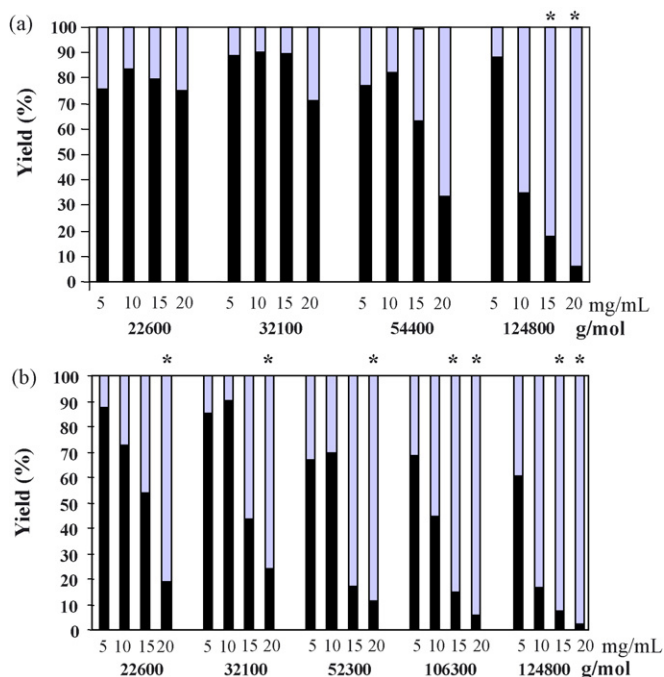


Fig. 3. Nanoparticle (black column) and polymeric aggregate (grey column) yields as a function of molar mass of PLA at different polymer concentrations in acetone (a), in THF (b). (*) Asterisks indicate nanoprecipitation experiments which led to polymer mass fractionation between nanoparticles and polymeric aggregates.

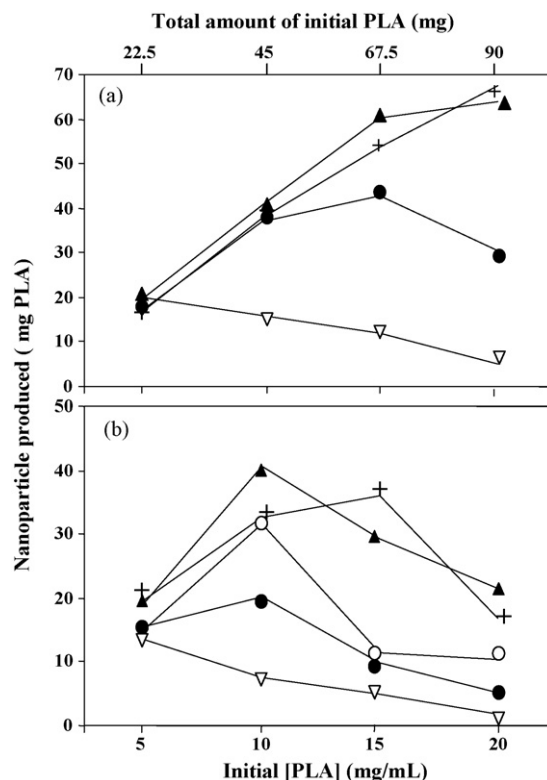


Fig. 4. Amounts of PLA recovered as nanoparticles as a function of initial PLA concentration in acetone (a) and in THF (b); PLA₂₂₆₀₀ (+), PLA₃₂₁₀₀ (▲), PLA₅₂₃₀₀ and PLA₅₄₄₀₀ (●), PLA₁₀₆₃₀₀ (○), PLA₁₂₄₈₀₀ (▽). Total amounts of polymer (mg) are reported on the top axis. Lines are used as guides for eyes. Relative error does not exceed 10%.

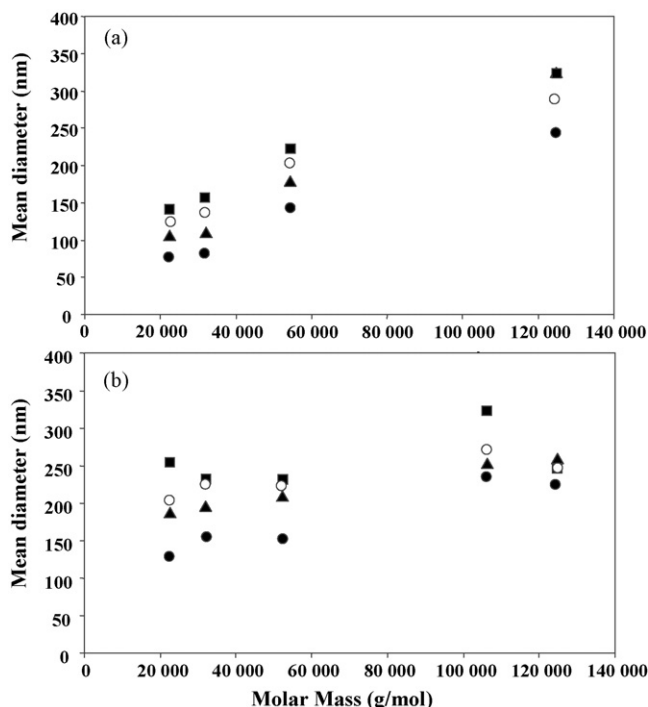


Fig. 5. Mean hydrodynamic diameter of nanoparticles separated by centrifugation as a function of PLA molar mass in acetone (a) and in THF (b) at different polymer concentrations. 5 mg/ml (●), 10 mg/ml (▲), 15 mg/ml (○), 20 mg/ml (■).

acetone than with THF. Whatever the PLA concentration and the solvent, the diameter of nanoparticles was always between 75 and 325 nm, and the polydispersity index was always less than 0.3. Nanoparticles with a diameter of less than 100 nm could only

be prepared from acetone solutions of PLA₂₂₆₀₀ and PLA₃₂₁₀₀ at 5 mg/ml. The polydispersity index was also the lowest for these nanoparticle preparations, indicating a better homogeneity of the preparation. At the same molar mass and PLA concentration in the solution, the particles obtained from acetone solution were always smaller than the particles obtained from THF solutions.

5.3. Molar mass determination

For each nanoprecipitation experiment, the molar mass of the initial PLA and of the polymer contained in the recovered nanoparticles and aggregates were analyzed to determine any changes in the molar mass of the PLA, which would appear as a shift of the elution peak. Fig. 6 gives a selection of chromatograms obtained for the initial PLA and of the polymer fractions constituting the corresponding nanoparticles and polymeric aggregates.

Results related to low molar mass PLAs were exemplified by the case of PLA₅₄₄₀₀ (from acetone) and PLA₅₂₃₀₀ (from THF) whereas PLA₁₂₄₈₀₀ was characteristic of high molar mass polymers. Fig. 6a shows that the molar mass of the initial PLA₅₄₄₀₀ and of the corresponding nanoparticles obtained by nanoprecipitation of a solution in acetone at the concentration of 5 mg/ml. In this preparation, the yield of nanoparticle formation was high (78%) and there were not enough aggregates to perform the GPC analysis on this fraction. The chromatogram of the PLA of the nanoparticles was exactly superimposed upon that of the initial PLA₅₄₄₀₀. When nanoprecipitation was performed in acetone at a concentration of 20 mg/ml, the polymeric aggregate fraction could be analyzed. Initial PLA, PLA in nanoparticles and PLA in aggregates showed superimposed chromatograms (Fig. 6c),

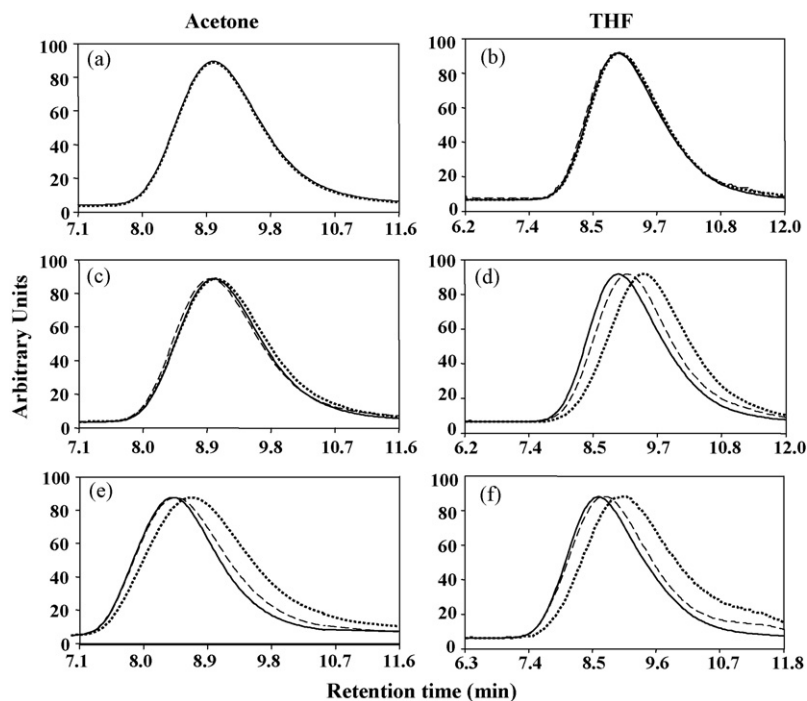


Fig. 6. High-performance gel permeation chromatograms of initial PLA (full line, —) and of PLA recovered from nanoparticles (dotted line, ···) and from polymeric aggregates (dashed line, ---) after nanoprecipitation in acetone (left-hand column): (a) PLA₅₄₄₀₀ at 5 mg/ml, (c) PLA₅₄₄₀₀ at 20 mg/ml, (e) PLA₁₂₄₈₀₀ at 20 mg/ml or in THF; (right-hand column): (b) PLA₅₂₃₀₀ at 5 mg/ml, (d) PLA₅₂₃₀₀ at 20 mg/ml, (f) PLA₁₂₄₈₀₀ at 20 mg/ml.

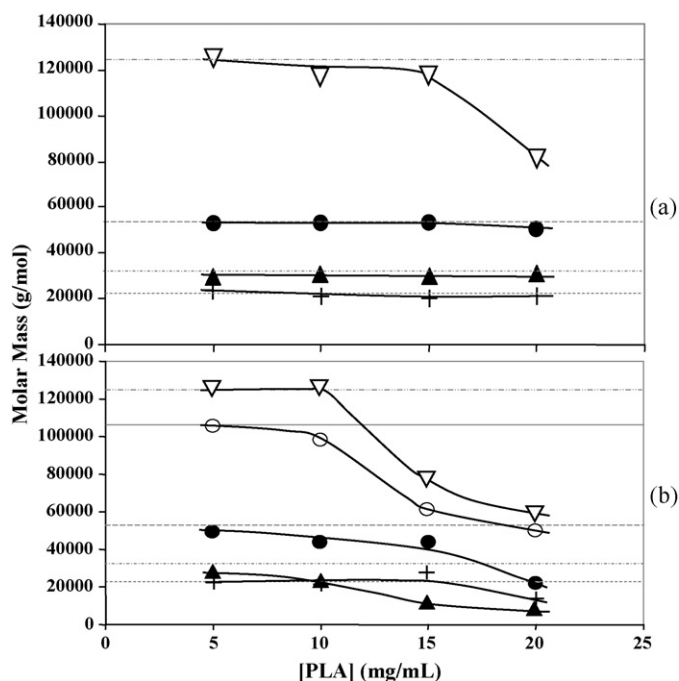


Fig. 7. Weight average molar mass of PLA recovered from the nanoparticle fraction as a function of the initial PLA concentration in acetone (a) and THF (b). PLA₂₂₆₀₀ (+), PLA₃₂₁₀₀ (▲), PLA₅₂₃₀₀ and PLA₅₄₄₀₀ (●), PLA₁₀₆₃₀₀ (○), PLA₁₂₄₈₀₀ (▽).

indicating that PLA₅₄₄₀₀ formed nanoparticles or bulk precipitate indifferently without molar mass selection. Fig. 6b shows that same result was obtained by nanoprecipitation of PLA₅₂₃₀₀, at 5 mg/ml in THF. However, a clear difference in the molar mass of the PLA recovered from the nanoparticles was observed after nanoprecipitation of PLA₅₂₃₀₀ from THF at 20 mg/ml compared with the characteristics of the initial PLA (Fig. 6d). When a PLA of a higher initial molar mass was used (PLA₁₂₄₈₀₀), this phenomenon was seen with both acetone and THF (Fig. 6e and f). The increase in retention times of the nanoparticle fractions suggested that nanoparticles could be formed only from low molar mass polymer chains while others precipitated as aggregates (Fig. 6d and f). This selection seemed to occur not only when initial PLA had a molar mass distribution centered on 124800 but also when the polymer concentration was increased even if its initial average molar mass was lower.

Fig. 7 summarizes the molar mass of the PLA recovered from the nanoparticles plotted as a function of the initial PLA concentration for the whole range of experimental conditions used. At low concentrations (5–15 mg/ml in acetone and 5–10 mg/ml in THF), the PLA recovered in the nanoparticles had the same molar mass than the initial PLA. However, a decrease of the molar mass of the PLA forming the nanoparticles was clearly seen when nanoprecipitation was performed with PLA of high molar mass (PLA₁₂₄₈₀₀ in acetone and PLA₅₄₄₀₀ and PLA₁₂₄₈₀₀ in THF) and when the PLA concentration increased (20 mg/ml in acetone, 15–20 mg/ml in THF). This molar mass selection was more pronounced in THF than in acetone and, when it was observed (see asterisk in Fig. 3a and b), the yield of nanoparticles was always low (less than 25%). On the other hand, under the

conditions giving the highest yield of nanoparticle production (PLA₂₂₆₀₀ and PLA₃₂₁₀₀), in most cases the molar mass of the PLA in the nanoparticles equalled the molar mass of the initial PLA.

6. Discussion

If nanoparticles are to be produced by nanoprecipitation on an industrial scale, it is necessary to find means of calibrating their size and optimizing the yield. In the present study we investigated some variables which could affect these parameters. Thus, we prepared nanoparticles from PLA of molar masses between 22600 and 124800 g/mol from acetone and THF solutions at different concentrations (5–20 mg/ml), using two volumes of aqueous phase for one volume of organic solvent and standardized nanoprecipitation conditions.

In agreement with the observations of Thioune et al., 1997 and Galindo-Rodriguez et al., 2004 on the preparation of nanoparticles from hydroxypropyl methylcellulose phthalate and polymethacrylic acid copolymers, increasing the concentration of polymer in the organic solvent led to formation of larger nanoparticles with a lower yield of fabrication. From our study, it appeared that the optimal concentration of polymer in the dispersed phase to obtain high yields of small particles was more influenced by the molar mass of the polymer than by its concentration. Nanoparticles with hydrodynamic diameters below 100 nm could only be prepared with PLA of low molar masses (PLA₂₂₆₀₀ and PLA₃₂₁₀₀). From the literature data (Niwa et al., 1993; Gref et al., 1994; Lannibois et al., 1997; Murakami et al., 1999, 2000; Chorny et al., 2002; Peltonen et al., 2003), small nanoparticles are usually obtained by nanoprecipitation when surfactants or polyethyleneglycol diblock copolymers are added to the formulation. Although no surfactant was added to our formulations, low molar mass PLA might have certain surface active properties which enhanced the formation of small polymer particles during nanoprecipitation. This hypothesis is supported by the fact that the hydrophilicity of PLA has been reported to be affected by the type of catalyst used during its synthesis. All the PLA polymers used in our study were synthesized using zinc metal ring-opening polymerization, which leads to the production of PLA with polar chain ends bearing free carboxylic groups (Vert et al., 1998). This polar groups grafted onto the hydrophobic backbone confers an amphiphilic character to PLA chains which is then closely linked to the chain length: the lower the PLA molar mass, the higher their hydrophilic/hydrophobic balance and hence their surface active properties, leading to the production of smaller particles. Due to their lower amphiphilic properties, long PLA chains could not form nanodispersed systems with high yields so easily even at rather low concentrations of PLA. This hypothesis is also supported by the observation that nanoparticles were formed by the precipitation of PLA chains of a quite well defined molar mass. A selection of molar mass of PLA during nanoprecipitation is not totally surprising because one established method for the fractionation of polymers used in mass-sieving is the iterative precipitation in non-solvent media (Fontanille and Gnanou, 2002). Thus, when the average molar mass of the initial PLA differed too much from the optimal value,

the yield of nanoparticle production decreased because only a fraction of the polymer chains present participated in the formation of nanoparticles. The remaining chains formed aggregates, resulting in a poor yield of nanoparticle production.

To further investigate the influence of the amphiphilicity of the PLA, a nanoprecipitation experiment was carried out with a small but more hydrophobic PLA (molar mass 14400 g/mol from Boeringer Ingelheim, *PLA₁₄₄₀₀) which was synthesized using Sn octanoate instead of zinc metal as catalyst. In this case, the chain ends of PLA are esterified by octanoic acid and the resulting polymer contains hydrophobic low molar mass by-products (Vert et al., 1998). As expected, the Huggin's k' reached a value of 1 with *PLA₁₄₄₀₀ which was quite different from the values of k' (0.5–0.6) evaluated for the series of PLA studied here (Table 2). After nanoprecipitation, the diameters of the nanoparticles were much higher with *PLA₁₄₄₀₀, whatever the concentration, than those obtained with the smallest PLA of the homologous series used in the present work, PLA₂₂₆₀₀. For instance, at a concentration of 5 mg/ml, the diameters of the nanoparticles obtained by the nanoprecipitation of *PLA₁₄₄₀₀ were 147 nm (acetone) and 243 nm (THF), whereas the corresponding diameters were 76 nm (acetone) and 129 nm (THF) after nanoprecipitation of PLA₂₂₆₀₀. This demonstrated that PLA nanoprecipitation from acetone and THF depended on the structure of the polymeric chains and their amphiphilic behaviour which govern their interactions with the organic solvents and in turn their ability to form nanodispersed precipitates in water. It may be assumed that, during the inter-diffusion of acetone or THF in water, the interface between the polymer organic solution and water was transiently stabilized, in favour of fine dispersion of the two phases. This is directly related to the nature of the PLA chain ends and hence to the method of PLA synthesis.

Nevertheless, whatever the molar masses and the concentrations of the PLA, the nanoparticles obtained from acetone solutions were always smaller than those prepared from THF. This is in agreement with the observation of Thioune et al., 1997 suggesting that the use of a more polar solvent led to the formation of smaller nanoparticles. Indeed, this was confirmed by the viscosity measurements leading to a lower Huggin's coefficient k' for acetone and by the exponent of 0.5 found in the Mark–Houwink's equation indicating that acetone is a theta solvent for PLA. It therefore appeared that good polymer solvents were preferable to optimize nanoparticle production and characteristics.

The role of the polymer–solvent interactions in the nanoprecipitation process could be better understood on the basis of the intrinsic viscosity values. The intrinsic viscosity of a polymer in solution reflects the mean hydrodynamic volume occupied by the polymer chains in a given solvent. For flexible chains in random coil conformation, like PLA under the experimental conditions of this study, this volume includes the volume fraction of the polymer solution corresponding to the statistical sphere in which the chain moves as an independent entity. In the absence of specific polymer–polymer interactions, provided the polymer concentration leads to a total volume fraction occupied by the chains smaller than the total solution volume, the chains

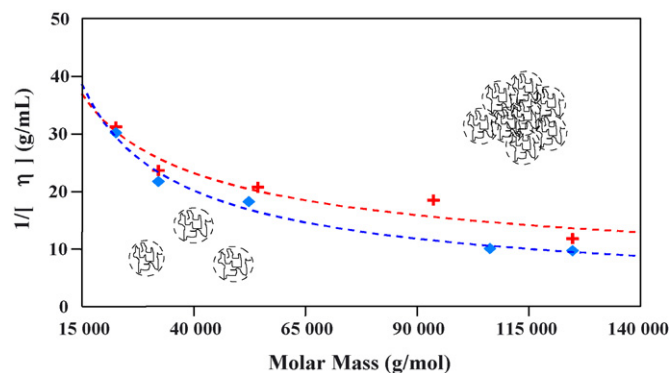


Fig. 8. Plot of the inverse of intrinsic viscosity as a function of PLA molar mass in acetone (+) and THF (♦) at 22 °C.

remain independent and no overlapping of the coils occur; this is the dilute solution regime. A reasonable approximation of the concentration limit beyond which the chains overlap is given by the inverse of the intrinsic viscosity. This corresponds to the concentration at which the total volume of the polymer solution is equal to the sum of the volume fractions occupied by the polymer coils. Fig. 8 shows variations of $1/[\eta]$ as a function of PLA molar mass in acetone and THF solution. First, it can be seen that the boundary between dilute and semi-dilute solution regimes differs slightly between acetone and THF. The former shifts coil overlapping towards higher PLA concentrations, in agreement with its behaviour as a theta solvent for PLA. The second piece of interesting information provided by Fig. 8 is that the best nanoparticle yields from a given PLA molar mass were obtained at polymer concentrations in the organic solvent below the critical concentration corresponding to the beginning of the semi-dilute regime; the more dilute the polymer, the better the yield. This is accompanied by a reduction in the nanoparticle diameter and a decrease of the polydispersity with lower molar masses and lower polymer concentrations, which could be due to a small effect of the viscosity of the polymer solution (Galindo-Rodriguez et al., 2004). In contrast, organic solutions of polymer at concentrations above the boundary between the dilute and semi-dilute regimes lead to dramatically reduced yields and predominance of bulk aggregation of the polymer. These observations suggest that upon pouring of the PLA organic solution into water, diffusion of the non-solvent leads to the association of the polymer chains and their passage into the solid state according to two different processes depending on the regime to which the organic solution of PLA belongs. In the dilute regime, the PLA chains are independent and separated by free solvent so that water penetration in the regions between the chains can isolate polymer clusters of definite sizes, which are all the smaller as the polymer is more dilute. When the polymer concentration increases, the fraction of organic solvent not involved in solvating the polymer decreases and leads to the increase in the cluster size until the semi-dilute regime is reached. At this stage, the chains overlap and water diffusion inevitably provokes bulk precipitation of most of the polymer.

This study has demonstrated that the transitory coexistence of water-rich regions and polymer-rich solvent regions at a nano-

metric scale in the dilute regime are necessary for the formation of nanoparticles. This is in agreement with the proposed explanations of the formation of nanoparticles by either the “Marangoni” or the “Ouzo effect” (Murakami et al., 1999; Ganachaud and Katz, 2005). During nanoprecipitation, the stability of the transient interface which forms between the PLA solution and water may be improved because of the polarity of PLA. This allows formation of clusters which become smaller as interface curvature increases, which happens as the surface activity of PLA becomes higher and, to a certain extent, as the PLA molar mass becomes lower. Indeed, short chains PLA molecules were used as surfactant in mixtures with high molar mass PLA to prepare self stabilized microparticles in another study (Carrio et al., 1995).

7. Conclusion

In summary, these results lead to the conclusion that for a well defined polymer it is possible to select the best formulation for calibrated nanoparticles in terms of size and yield. The choice of a good solvent of the polymer is fundamental. In fact, the quality of the nanoparticles depends on the polymer–solvent interactions. **Once a good solvent of the polymer has been chosen, structural properties of the polymer (chain length, chain ends, surface active properties determined by the polarity of the chain ends) are the main parameters which control size and fabrication yield.** Thus, amphiphilic polymers are preferable because they remove the need to add surfactant to stabilize the interface. In the dilute regime, low molar masses of PLA with carboxylic end-groups produce small calibrated nanoparticles at high yields. Polymer in the semi-dilute solution regime leads to the selection of the PLA chains which are able to form nanoparticles and consequently to low yields of production. This effect is especially pronounced for high molar mass PLA at high concentrations. For a given molar mass and organic solvent it is important to optimize the polymer solution in order to be at the boundary between the dilute and semi-dilute regime. The discrimination between these regimes can be made by the simple procedure of measuring the intrinsic viscosity of the polymer solution. For instance, it can be deduced from Fig. 8 that optimal conditions for the preparation of PLA nanoparticles will be obtained using a solution of PLA in acetone at a concentration of 20 mg/ml with a PLA showing a molar mass below 40 000 g/mol.

Acknowledgements

The authors wish to thank Patrick Couvreur and Florence Agnely for stimulating discussions, Celine Fontenelle and Sara Kaffache for technical assistance, and Jean Louis Grossiord for assistance in the viscosity measurements. This work was supported by the CNRS.

References

Agrawal, A., Saran, A.D., Rath, S.S., Khanna, A., 2004. Constrained nonlinear optimization for solubility parameters of poly(lactic acid) and poly(glycolic acid): validation and comparison. *Polymer* 45, 8603–8612.

- Allen, T.M., Chonn, A., 1987. Large unilamellar liposomes with low uptake into the reticuloendothelial system. *FEBS Lett.* 223, 42–46.
- Bagley, E.B., Nelson, T.P., Scigliniano, J.M., 1971. Three-dimensional solubility parameters and their relation to internal pressure measurements in polar and hydrogen bonding solvents. *J. Paint Technol.* 43, 35–42.
- Belbella, A., Vauthier, C., Fessi, H., Devissaguet, J.P., Puisieux, F., 1996. In vitro degradation of nanospheres from poly(D,L-lactides) of different molecular weights and polydispersities. *Int. J. Pharm.* 129, 95–102.
- Brannon-Peppas, L., Blanchette, J.O., 2004. Nanoparticle and targeted systems for cancer therapy. *Adv. Drug Deliv. Rev.* 56, 1649–1659.
- Burrell, H., 1975. In: Brandrup, J., Immergut, E.H. (Eds.), *Polymer Handbook*, second ed. J. Wiley & Sons, Inc., New York, pp. IV 337–IV 359.
- Carrio, A., Schwach, J., Coudane, J., Vert, M., 1995. Preparation and degradation of surfactant free PLGA microspheres. *J. Controlled Release* 37, 113–121.
- Chorny, M., Fishbein, I., Danenberg, H.D., Golomb, G., 2002. Study of the drug release mechanism from tyrophostin AG-1295-loaded nanospheres by in situ and external sink methods. *J. Controlled Release* 83, 389–400.
- De Jaeghere, F., Doelker, E., Gurny, R., 1999. Nanoparticles. In: Mathiowitz, E. (Ed.), *The Encyclopedia of Controlled Drug Delivery*. Wiley and Son, New York, pp. 641–664.
- Delair, T., 2004. Colloidal particles: elaboration from preformed polymers. In: Elaissari, A. (Ed.), *Colloidal Biomolecules, Biomaterials, and Biomedical Applications*. Marcel Dekker Inc., New York, pp. 329–347.
- Duclairoir, C., Nakache, E., Marchais, H., Orecchioni, A.M., 1998. Formation of gliadin nanoparticles: influence of the solubility parameter of the protein solvent. *Colloid Polym. Sci.* 276, 321–327.
- Fessi, H., Puisieux, F., Devissaguet, J.P., Ammoury, N., Benita, S., 1989. Nanocapsule formation by interfacial polymer deposition following solvent displacement. *Int. J. Pharm.* 55, R1–R4.
- Flory, P.J., 1953. *Principles of Polymer Chemistry*. Cornell University Press, Ithaca, New York.
- Flory, P.J., 1969. *Statistical Mechanics and Chain Molecules*. Interscience Pub., John Wiley & Sons Ed, New York, chapter 2, pp. 30–48.
- Fontanille, M., Gnanou, Y., 2002. *Chemistry and Physical-Chemistry of Polymers*. Dunod, Paris.
- Galindo-Rodriguez, S., Alleman, E., Fessi, H., Doelker, E., 2004. Physicochemical parameters associated with nanoparticle formation in the salting-out, emulsification-diffusion, and nanoprecipitation methods. *Pharm. Res.* 21, 1428–1439.
- Ganachaud, F., Katz, J.L., 2005. Nanoparticles and nanocapsules created using the Ouzo effect: spontaneous emulsification as an alternative to ultrasonic and high-shear devices. *Chem. Phys. Chem.* 6, 209–216.
- Govender, T., Stolnik, S., Garnett, M.C., Illum, L., Davis, S.S., 1999. PLGA nanoparticles prepared by nanoprecipitation: drug loading and release studies of a water soluble drug. *J. Controlled Release* 57, 171–185.
- Gref, R., Minamitake, Y., Peracchia, M.T., Trubetskoy, V., Torchilin, V., Langer, R., 1994. Biodegradable long-circulating polymeric nanospheres. *Science* 263, 1600–1603.
- Gref, R., Luck, M., Quellec, P., Marchand, M., Dellacharie, E., Harnish, S., Blunk, T., Muller, R.H., 2000. ‘Stealth’ corona-core nanoparticles surface modified by polyethylene glycol (PEG): influences of the corona (PEG chain length and surface density) and of the core composition on phagocytic uptake and plasma protein adsorption. *Colloids Surf. B: Biointerfaces* 18, 301–313.
- Gref, R., Couvreur, P., Barratt, G., Mysiakine, E., 2003. Surface-engineered nanoparticles for multiple ligand coupling. *Biomaterials* 24, 4529–4537.
- Huggins, M.L., 1942. The viscosity of dilute solutions of long-chain molecules. IV. Dependence on concentration. *J. Am. Chem. Soc.* 64, 2716–2718.
- Jain, R.A., 2000. The manufacturing techniques of various drug loaded biodegradable poly(lactide-co-glycolide) (PLGA) devices. *Biomaterials* 21, 2475–2490.
- Jain, R., Shah, N.H., Malick, A.W., Rhodes, C.T., 1998. Controlled drug delivery by biodegradable poly(ester) devices: different preparative approaches. *Drug Dev. Ind. Pharm.* 24, 703–727.
- Jeon, H.J., Jeong, Y.I., Jang, M.K., Park, Y.H., Nah, J.W., 2000. Effect of solvent on the preparation of surfactant-free poly(DL-lactide-co-glycolide) nanoparticles and norfloxacin release characteristics. *Int. J. Pharm.* 207, 99–108.
- Juliano, R.L., 1976. The role of drug delivery systems in cancer chemotherapy. *Prog. Clin. Biol. Res.* 9, 21–32.

- Lamprecht, A., Ubrich, N., Yamamoto, H., Schäfer, U., Takeuchi, H., Lehr, C.M., Maincent, P., Kawashima, Y., 2001. Design of rolipram-loaded nanoparticles: comparison of two preparation methods. *J. Controlled Release* 71, 297–306.
- Lannibois, H., Hasmy, A., Botet, R., Aguerre Chariol, O., Cabane, B., 1997. Surfactant limited aggregation of hydrophobic molecules in water. *J. Phys. II France* 7, 319–342.
- Lannibois-Drean, H., 1995. Des molécules hydrophobes dans l'eau: fabrication de nanoparticules par précipitation. Ph.D. Université Pierre et Marie Curie, Paris, France.
- Le Roy Boehm, A.L., Zerrouk, R., Fessi, H., 2000. Poly epsilon-caprolactone nanoparticles containing a poorly soluble pesticide: formulation and stability study. *J. Microencapsulation* 17, 195–205.
- Lemos-Senna, E., 1998. Contribution à l'étude pharmacotechnique et physico-chimique de nanosphères de cyclodextrines amphiphiles comme transporteurs de principes actifs. Ph.D. Université de Paris XI, Chatenay-Malabry.
- Leo, E., Brina, B., Forni, F., Vandelli, M.A., 2004. In vitro evaluation of PLA nanoparticles containing a lipophilic drug in water-soluble or insoluble form. *Int. J. Pharm.* 278, 133–141.
- Lu, Y., Chen, S.C., 2004. Micro and nano-fabrication of biodegradable polymers for drug delivery. *Adv. Drug Deliv. Rev.* 56, 1621–1633.
- Moghimi, S.G., Hunter, A.C., Murray, J.C., 2001. Long-circulating and target-specific nanoparticles: theory to practice. *Pharmacol. Rev.* 53, 283–318.
- Molceperes, J., Guzman, M., Arberturas, M.R., Chacon, M., Berges, L., 1996. Application of central composite designs to the preparation of polycaprolactone nanoparticles by solvent displacement. *J. Pharm. Sci.* 85, 206–213.
- Murakami, H., Kobayashi, M., Takeuchi, H., Kawashima, Y., 1999. Preparation of poly(DL-lactide-co-glycolide) nanoparticles by modified spontaneous emulsification solvent diffusion method. *Int. J. Pharm.* 187, 143–152.
- Murakami, H., Kobayashi, M., Takeuchi, H., Kawashima, Y., 2000. Further application of a modified spontaneous emulsification solvent diffusion method to various types of PLGA and PLA polymers for preparation of nanoparticles. *Powder Technol.* 107, 137–143.
- Niwa, T., Takeuchi, T., Hino, T., Kunou, N., Kawashima, Y., 1993. Preparations of biodegradable nanospheres of water-soluble and insoluble drugs with D,L-lactide/glycolide copolymer by a novel spontaneous emulsification solvent diffusion method, and the drug release behavior. *J. Controlled Release* 25, 89–98.
- Oppenheim, R.C., 1986. Nanoparticulate drug delivery systems based on gelatin and albumin. In: Guiot, P., Couvreur, P. (Eds.), *Polymeric Nanoparticles and Microspheres*. CRC Press, Boca Raton, FL, pp. 1–25.
- Panyam, J., Labhasetwar, V., 2003. Biodegradable nanoparticles for drug and gene delivery to cells and tissue. *Adv. Drug Deliv. Rev.* 55, 329–347.
- Peltonen, L., Koistinen, P., Hirvonen, J., 2003. Preparation of nanoparticles by nanoprecipitation of low molecular weight poly(l)lactide. *STP Pharma Sci.* 5, 299–304.
- Riesemann, J., Ullman, R., 1951. The concentration dependence of the viscosity of solutions of macromolecules. *J. Chem. Phys.* 19, 578.
- Skiba, M., Wouessidjewe, D., Coleman, A., Fessi, H., Devissaguet, J.P., Duchene, D., Puisieux, F., 1993. Préparation et application de nouveaux systèmes colloïdaux nanovésiculaires dispersibles à base de cyclodextrine, sous forme de nanosphères. Eur. Patent PCT application Fr 93/00594, 16 June.
- Södergård, A., Stolt, M., 2002. Properties of lactic acid based polymers and their correlation with composition. *Prog. Polym. Sci.* 27, 1123–1163.
- Stainmesse, S., Orecchioni, A.M., Nakache, E., Puisieux, F., Fessi, H., 1995. Formation and stabilization of a biodegradable polymeric colloidal suspension of nanoparticles. *Colloid Polym. Sci.* 273, 505–511.
- Sung, J.H., Lee, D.C., 2001. Molecular shape of poly(2-ethyl-2-oxazoline) chains in THF. *Polymer* 42, 5771–5779.
- Thioune, O., Fessi, H., Devissaguet, J.P., Puisieux, F., 1997. Preparation of pseudolatex by nanoprecipitation: Influence of the solvent nature on intrinsic viscosity and interaction constant. *Int. J. Pharm.* 146, 233–238.
- Trotta, M., Debernardi, F., Caputo, O., 2003. Preparation of solid lipid nanoparticles by a solvent emulsification-diffusion technique. *Int. J. Pharm.* 257, 153–160.
- Van Krevelen, D.W., Hoftyzer, P.J., 1976. *Properties of Polymers: their Estimation and Correlation with Chemical Structure*, second ed. Elsevier Scientific Publishing Company, Amsterdam-Oxford-New York.
- Vauthier, C., Fattal, E., Labarre, D., 2004. From polymer chemistry and physicochemistry to nanoparticulate drug carrier design and applications. In: Yaszemski, M.J., Trantolo, D.J., Lewandrowski, K.U., Hasirci, V., Altobelli, D.E., Wise, D.L. (Eds.), *Biomaterial Handbook-Advanced Applications of Basic Sciences and Bioengineering*. Marcel Dekker, Inc., New York, pp. 563–598.
- Vert, M., Schwach, G., Engel, R., Coudane, J., 1998. Something new in the field of PLA/GA bioresorbable polymers? *J. Controlled Release* 53, 85–92.